

MODELLING THE STEADY STATE CSR EMISSION IN LOW ALPHA MODE AT THE DIAMOND STORAGE RING

I.P.S. Martin, C.A. Thomas, Diamond Light Source, Oxfordshire, U.K.
 R. Bartolini, Diamond Light Source, Oxfordshire, U.K. and John Adams Institute,
 University of Oxford, U.K.

Abstract

The CSR emitted by short electron bunches can be of a stable or bursting nature, with transition between the two states characterised by a threshold current that depends on various machine parameters. Key to understanding this process is to develop an effective model that describes the way the electron bunch interacts with various impedance sources such as the CSR wakefield and surrounding vacuum chamber. In this paper we present the latest results of modelling the equilibrium distribution calculated using the Haissinski equation driven by different impedance models. The bunch lengthening with current, bunch profiles and CSR form factors derived from this model are compared to measured data for both positive and negative momentum compaction factor. Comparisons of the measured instability thresholds to theoretical predictions are also discussed.

INTRODUCTION

The emission of coherent synchrotron radiation (CSR) in rings is currently of great interest, both because of its use as a powerful source of THz radiation and as a valuable diagnostic tool for gaining insight into the complex underlying electron beam dynamics. At Diamond, this CSR emission has been studied using a Schottky Barrier Diode (SBD) [1], and more recently at the B22 Infrared Micro-spectroscopy beamline [2].

The CSR power at wavelength λ can be calculated from the number of electrons in the bunch n_e and the single particle spectrum $P_e(\lambda)$ using

$$P(\lambda) = P_e(\lambda)(n_e + f_\lambda n_e(n_e - 1)) \quad (1)$$

The form factor f_λ varies between 0 for an infinitely long, smooth bunch and 1 for a point source. If there is a local density modulation, this will enhance the form factor at the modulation wavelength; it is the form factor that allows the intensity of CSR emitted at any given wavelength to be determined.

The form factor is defined as the square of the Fourier transform of the longitudinal charge distribution $n(z)$,

$$f_\lambda = \left| \int_{-\infty}^{\infty} n(z) \exp(2\pi iz/\lambda) dz \right|^2 \quad (2)$$

and so the first step in understanding how the intensity and temporal CSR emission pattern will vary with bunch current is to determine $n(z)$ (equilibrium or otherwise). This distribution depends strongly upon the combined impedance of the CSR and vacuum chamber wakefields. In steady state, the impedance acts to cause a lengthening and distortion of the longitudinal profile which can enhance the Fourier components at shorter wavelengths compared to a Gaussian distribution [3]. Above a certain

threshold current, the impedance drives a micro-bunching instability [4], in which an initially small density modulation generates a CSR wakefield, which in turn acts back on the bunch and increases the density modulation. The geometric wakefields occur at sources of impedance such as cavities, tapers and other transitions. Real wakefields can be complex; in order to facilitate theoretical studies they are frequently approximated by simple models.

STEADY STATE CSR EMISSION

Modelling the Equilibrium Distribution

Using the coordinate system of [5], the normalised longitudinal electron distribution $\lambda(q)$ can be described by the solution of the Haissinski equation

$$\lambda(q) = \frac{1}{\kappa} \exp\left(-\frac{q^2}{2} \pm I_n \int_{-\infty}^q V_{ind}(q') dq'\right) \quad (3)$$

where $q = z/\sigma_z$ is the longitudinal coordinate and the normalised current I_n is given by

$$I_n = \frac{r_e N_b}{2\pi v_s \gamma \sigma_E} \quad (4)$$

In this study, the induced wakefield $V_{ind}(q)$ is approximated as the combination of a purely resistive term $R(I_n)$, a purely inductive term $L(I_n)$ and the shielded CSR wakefield W_{CSR} (using the parallel-plate model)

$$V_{ind}(q) = \left[R(I_n)\lambda(q) - L(I_n) \frac{d\lambda(q)}{dq} + \int_{-\infty}^{\infty} W_{CSR}(q - q')\lambda(q) dq' \right] \quad (5)$$

The inductive and resistive terms in Eq. 5 are modelled as functions of the beam current to account for the fact that as the bunch length and shape become distorted, different parts of the ring impedance will become emphasised [6].

Equation 3 is solved via numerical integration, with the particular values for $R(I_n)$ and $L(I_n)$ for any given storage ring configuration determined as best fit values using bunch profiles extracted from streak camera measurements. Before the fitting is performed, the streak camera profiles are deconvolved with the camera point spread function in order to ensure best match between model and measured data. Using this technique, longitudinal profiles and form factors can be determined for arbitrary bunch currents, free from the unavoidable high-frequency noise present in the measured profiles.

Electron Bunch Profiles

First trials of the fitting technique were performed using streak camera measurements recorded on lattices

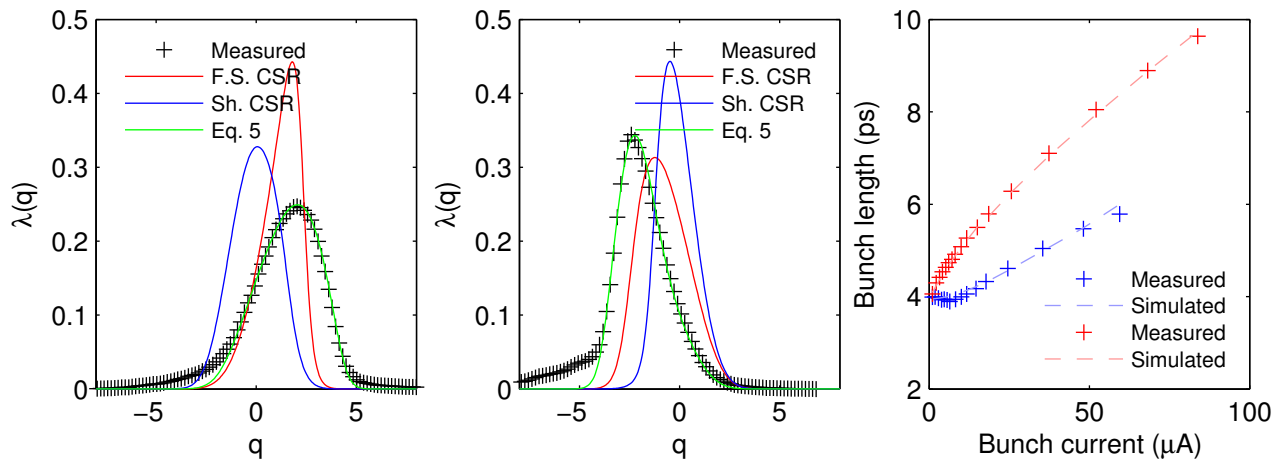


Figure 1: (left) Bunch profile for $\alpha_l = +1 \times 10^{-5}$, $V_{RF} = 1.5\text{MV}$, $I_b = 25\mu\text{A}$. (centre) Bunch profile for $\alpha_l = -1 \times 10^{-5}$, $V_{RF} = 1.5\text{MV}$, $I_b = 25\mu\text{A}$. (right) Bunch length as a function of current for positive (red) and negative (blue) α_l .

with $\alpha_l = \pm 1.0 \times 10^{-5}$ and $V_{RF} = 1.5\text{MV}$. Profiles were recorded for increasing values of bunch current, and Eq. 3 was solved firstly using only the free-space CSR wakefield, then with the shielded CSR term and finally using Eq. 5. Results are shown in Fig. 1. The measured bunch profiles deviate significantly from those calculated using only the free-space or shielded CSR wakefields, with the improved match for Eq. 5 clearly evident. For operation with positive α_l , the bunch length grows immediately and the profile becomes more bulbous, leaning towards the head of the bunch. In contrast, for negative α_l the bunch profile becomes sharper, growing more slowly and leaning towards the bunch tail.

Electron Bunch Form Factor

Having determined effective values for $R(I_n)$ and $L(I_n)$, the corresponding form factors for the simulated profiles can be found using Eq. 2. These can be used to calculate the expected CSR emitted in the 60 to 90GHz bandwidth for each bunch current and compared to measurements taken with the SBD. The results for $\alpha_l = -1 \times 10^{-5}$ and $V_{RF} = 1.5\text{MV}$ are shown in Fig. 2. As can be seen, the power emitted shows an initial quadratic increase with bunch current consistent with true CSR emission. Above $\sim 15\mu\text{A}$, the bunch length begins to grow and f_l in this bandwidth is reduced, resulting in the increase in power dropping below quadratic. This reduction in f_l due to bunch lengthening is partially mitigated by the leaning of the bunch profile, such that the CSR power calculated from the simulated profiles closely match the measured data. This supports the view that, in this current range, the SBD data can be described purely in terms of a potential well distortion.

Similar calculations were performed using streak camera data measured with $\alpha_l = -4.5 \times 10^{-6}$ and $V_{RF} = 2.2\text{MV}$ with an 800 bunch fill pattern. The form factors for bunch currents of $1.7\mu\text{A}$, $4.0\mu\text{A}$ and $6.1\mu\text{A}$ are shown in Fig. 3. These conditions replicate those used during measurements taken on the IR beamline B22 [2, 7]. In contrast to the SBD results, the power measured at B22

shows an above quadratic scaling with bunch current [2], consistent with the rise in f_l shown in Fig. 3. However, despite the fact that the simulated bunch profiles show good agreement with the measured streak camera images, the derived form factors are too small to explain in full the spectra measured by the beamline (see Fig. 1 in [7]). The bunch currents in this case are well below the measured single bunch instability thresholds; however, experimentally we find the multi-bunch instability threshold to be lower than the single bunch equivalent, so one possible explanation for the discrepancy is that small scale micro-bunching was producing an enhanced f_l .

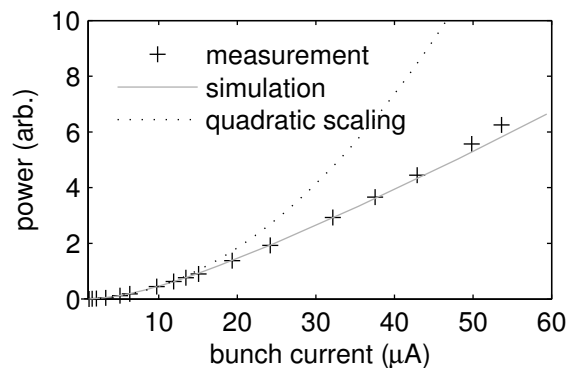


Figure 2: CSR power measured with the SBD.

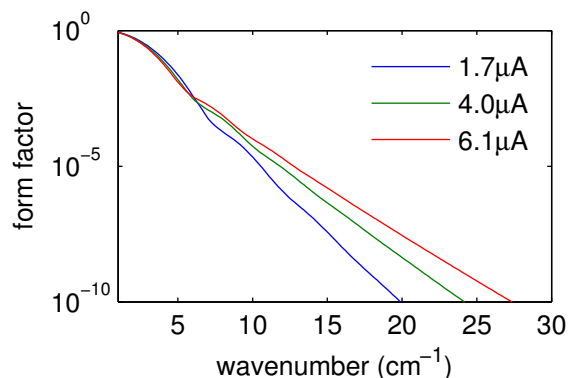


Figure 3: f_l calculated for $\alpha_l = -4.5 \times 10^{-6}$, $V_{RF} = 2.2\text{MV}$.

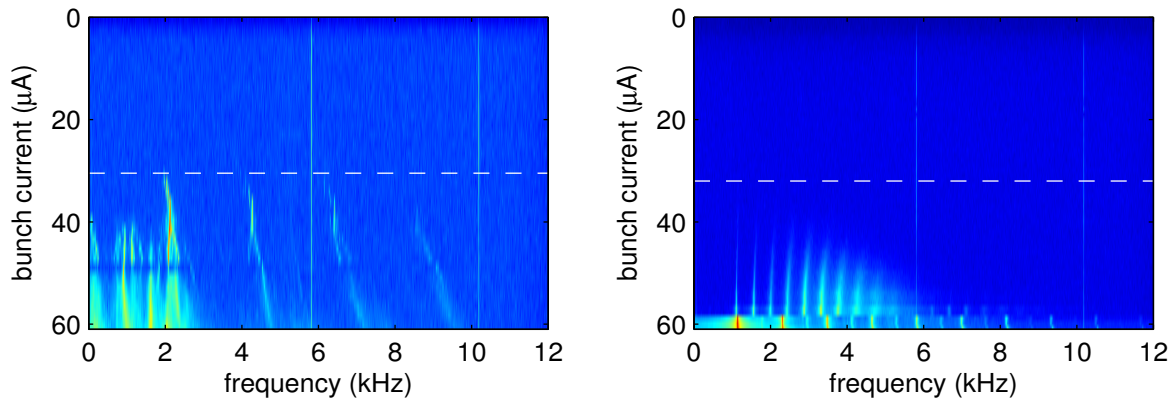


Figure 4: Spectrograms showing the temporal modulation in signal strength from the SBD as a function of single bunch current. Shown are examples measured at VRF = 3.4MV for with $\alpha_l = +1.0 \times 10^{-5}$ (left) and $\alpha_l = -1.0 \times 10^{-5}$ (right).

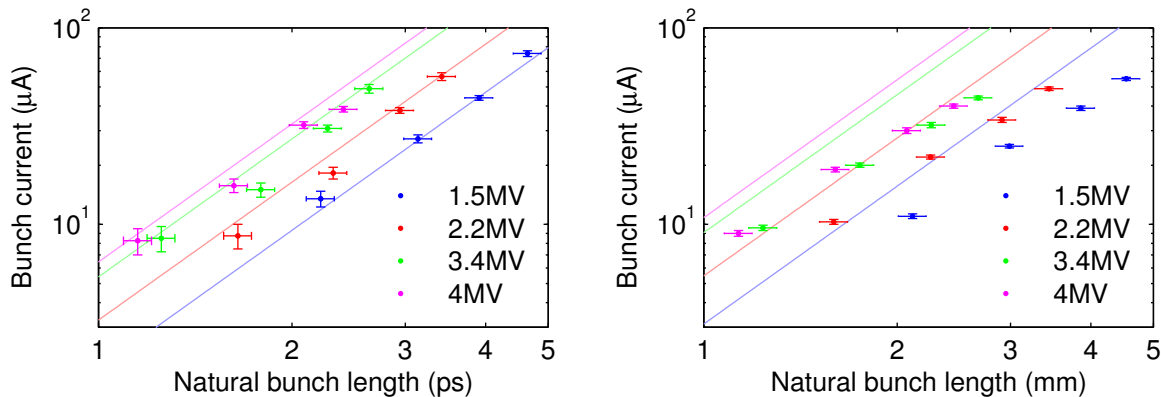


Figure 5: Measured instability thresholds as a function of single bunch current for positive (left) and negative α_l (right). Solid lines are calculated using Eq. 6 assuming $\lambda = \sigma_0$.

INSTABILITY THRESHOLDS

The free-space CSR instability threshold introduced in [4] can be expressed as [8]

$$I_{\text{thresh}}(\lambda) = \frac{(2\pi)^{1/6} ec \gamma}{K^{2/3} \tau_e \rho^{1/3}} \alpha_c \sigma_E^2 \frac{\sigma_0}{\lambda^{2/3}} \quad (6)$$

where the numerical factor K was calculated to be 2.0 for positive α_l and 0.92 for negative α_l respectively. According to this model, the threshold current is wavelength dependent, with the bunch becoming unstable to longer wavelengths first. To simplify the analysis, λ is frequently replaced with the natural bunch length σ_0 . From Eq. 6, the threshold current is expected to be higher for negative α_l .

At Diamond, the instability threshold is taken to be the point when sidebands first appear in the spectrum of the temporal modulation in signal strength from the SBD. Typical examples are shown in Fig. 4, in which the behaviour in positive and negative α_l is shown to be strikingly different. Measured instability thresholds are given in Fig. 5. When defined in this way, the threshold is found to be much lower than the point when bursts of radiation appear, and is roughly equally for both positive and negative α_l . This is in contradiction with Eq. 6; however, the steady state analysis of the previous section demonstrates that, at Diamond, the CSR impedance is not sufficient to describe the electron dynamics in full.

CONCLUSIONS

A method has been described for calculating the stationary electron distribution when under the influence of combined CSR and geometric wakefields. The model accurately reproduces measured bunch profiles and bunch lengthening curves, and gives insight into the total CSR power and spectra measured with the SBD and at B22. It is anticipated the model can be used as the basis for further in-depth time dependent studies. Micro-bunching instability thresholds have been presented for a wide range of machine conditions, and the different behaviour in positive and negative α_l has been highlighted.

The authors would like to thank P. Kuske for many illuminating discussions on this topic, along with G. Wuestefeld, J. Feikes, M. Ries, V. Judin and C. Evain. Contributions to the CSR studies by G. Cinque, G. Rehm, A. Morgan, and M. Frogley are also gratefully received.

REFERENCES

- [1] G. Rehm et al., DIPAC'09, TUPD32, (2009).
- [2] G. Cinque et al., Rendiconti Lincei **22**, p. 33, (2011).
- [3] F. Sannibale et al., PRL **93**, 094801, (2004).
- [4] G. Stupakov, S. Heifets, PRST-AB **5**, 054402, (2002).
- [5] K. Bane et al., PRST-AB **13**, 104402, (2010).
- [6] K. Bane, SLAC-PUB-5177, (1990).
- [7] R. Bartolini et al., IPAC'11, THPC068, (2011).
- [8] J.M. Byrd et al., PRL **89**, 224801, (2002).